

Impact of Various pH Levels on 4-Methyl Catechol Treatment of Wood

Md. Tipu Sultan,^{a,*} Md. Rezaur Rahman,^a Sinin Hamdan,^b Josephine Chang Hui Lai,^a Zainal Abidin Talib,^c and Fahmi Asyadi Bin Md Yusof^d

Four types of treated wood (TW) were prepared by the impregnation of solid wood each with a solution of 4-methyl catechol at pH 8, a solution of 4-methyl catechol at pH 9, a solution of 4-methyl catechol at pH 10, and a solution of 4-methyl catechol at pH 11. These TW were characterized by Fourier transform infrared spectroscopic, X-ray diffraction (XRD), scanning electron microscopic, 3-point bending, free-free-vibration, and thermo-gravimetric analysis. FT-IR result showed that TW had more than one carbonyl absorbance band between 1745 and 1690 cm^{-1} , while raw wood had only one carbonyl absorbance band in this regard. TW at pH levels of eight and nine showed higher crystallinity index (Cl_{XRD}) than that of raw wood. The SEM micrograph of TW at pH 8 had a smoother surface compared with other treated wood and raw wood. The modulus of elasticity (MOE), and modulus of rupture (MOR) of TW at pH 8 and pH 9 significantly increased. The raw wood exhibited a higher water uptake compared with the TW. The TGA results showed that TW were thermally less stable between 267 and 400 °C than raw wood.

Key words: TW; Mechanical properties; TGA; XRD; SEM; pH

Contact information: a: Department of Chemical Engineering and Energy Sustainability, Faculty of Engineering, Universiti Malaysia Sarawak, 94300 Kota Samarahan, Sarawak, Malaysia; b: Department of Mechanical Engineering, Faculty of Engineering, Universiti Malaysia Sarawak, 94300 Kota Samarahan, Sarawak, Malaysia; c: Department of Physics, Faculty of Science, Universiti Putra Malaysia, 43400 UPM Serdang, Selangor, Malaysia, and; d: Department of Polymer Engineering Technology, University of Kuala Lumpur, Malaysia; *Correspondent author: tipuchem75@gmail.com

INTRODUCTION

Wood is a combination of cellulose, hemicellulose, and lignin. One can regard hemicellulose as a binder that holds crystalline hydrophilic cellulose together with the amorphous hydrophobic lignin. Since the beginning of human civilization, wood has been used to make shelters, boats, wheels, and construction tools. Recently, scientists and economists have shown a preference for wood over non-renewable synthetic materials because of its renewability. Wood lowers both the cost of the materials and energy consumption, and it recycles better than glass material (O'Donnell *et al.* 2004; Ku *et al.* 2011). Wooden materials have long been used to construct buildings because of their excellent specific strength, high specific modulus, and aesthetic properties. The plastics industry uses wood sawdust as reinforcement to improve the stiffness of composites (Stark and Rowlands 2003). One of the examples of wood usage is in musical instruments due to the better sound, color, and acoustic properties. Besides, the cracks can be well determined through the natural frequency of a wooden beam (Landis and Navi 2009).

The main drawbacks of wood are that it is dimensionally unstable, it is susceptible to microorganism attack, and that it absorbs water from the environment in its cell walls and cavities because of hydrophilic and capillarity properties (Singh and Mohanty 2007; Belgacem and Gandini 2008; Kojiro *et al.* 2008; Mohebbi and Militz 2010; Mattos *et al.* 2014; Redman *et al.* 2016). Wood also discolors when used indoors because of the oxidation of lignin (Sahin and Mantanis 2011).

Recently, wood has been treated with a variety of chemicals, such as styrene, epoxy resins, urethane, phenol formaldehyde resin, methyl methacrylate (MMA), acrylic, and vinyl monomers, and to improve its physical, hydrophobic, mechanical, and biological properties (Sultan *et al.* 2016; Rahman *et al.* 2012). Thermosetting and thermoplastic monomer wood composites have shown certain improvements in wood properties, with some limitations (Li *et al.* 2011). Thermosetting-related polymers, such as phenolic resins, urea-formaldehyde, and melamine-formaldehydes, show better compressive strength, moisture-shrinking, and swelling behaviors. However, wood treated with these types of polymers may be more brittle and displays only marginal improvement in morphological properties. Thermoplastic-type monomers, such as acrylate, styrene, and methacrylate, slightly improve the dimensional stability because there is no bond formation between the hydroxyl groups of cellulose and the monomer. These polymers simply fill the void spaces within the wood structure (Esteves *et al.* 2014). Poor chemical and physical interfacial interactions between the wood surface and chemical are the most important mechanisms of bond failure (Rowell 2012).

NaOH-treated wood performs better than wood treated with thermosetting-related polymers. In general, wood's strength is affected when it is treated with an acid or a base at high temperatures. Alkaline solutions are more destructive to wood fibers than acidic solutions because wood absorbs alkaline solutions more readily than acidic solutions (Junior *et al.* 2010). Acids with pH values above 2 and bases with pH values below 10 do not greatly degrade wood fibers over short periods at low temperatures (Kollmann and Cote 1968). Undesirable water uptake also can be controlled by removing lignin and hemicellulose (Glasser *et al.* 1999).

Mechanical properties and the spiral angle of alkali-treated wood decrease after the removal of lignin-hemicellulose resin and pigment from the wood cell. The resulting surface of the wood is rougher, with high aspect ratio fibers to enhance the mechanical interlocking with external polymer (Mohanty *et al.* 2001; Barreto *et al.* 2011; Rahman *et al.* 2011). Natural fibers treated by NaOH increase their molecular orientation, thus increasing their stiffness. During alkali treatment, the fibers swell, kink, and curl, and the shape of the cell cavity changes from flat to oval (Wang *et al.* 2016). In addition, alkali-treated wood has an increased crystallinity index, which results in stiff wood and lower water absorption (Ghali *et al.* 2009).

Polymer-treated wood combines the performance and cost attributes of both wood and thermoplastics. Therefore, after chemical treatment of fast-growing and low-quality wood, it can be used effectively for sustainable development (Rahman *et al.* 2010a; Islam *et al.* 2012a; Devi and Maji 2013). To improve the adhesion and compatibility of polymer to cellulose, wood samples can be chemically pretreated with a 5% alkaline NaOH solution, then treated with an MMA/ST monomer mixture to manufacture pretreated wood polymer composite (Islam *et al.* 2012a).

Alkaline-treated fibers show better thermal stability than untreated fibers because of a decrease in hemicellulose and an increase in residual char formation (Das and Chakrabarty 2008). However, there has been no work on tropical wood impregnation

with 4-methyl catechol monomer at various pH levels.

In this study, raw wood was treated with 4-methyl catechol at various pH levels to increase its mechanical and hydrophobic properties. 4-methyl catechol was chosen to be used to treat wood, as 4-methyl catechol can be polymerized in presence of pH above 7 (Jha and Halada 2011). The thermal stability is also reported.

EXPERIMENTAL

Materials

Defect-free and straight-grained raw wood (RW) of Kumpang (*Gymnacranthera eugenifolia*) was obtained from Sematan (Sarawak, Malaysia). The chemicals used to produce TW were 4-methyl catechol, methanol, and sodium hydroxide. 4-methyl catechol ($\geq 95\%$) as a monomer and methanol ($\geq 99\%$) as a solvent were supplied by Sigma Aldrich (St. Louis, MO). Sodium hydroxide was supplied by Merck KgaA (Darmstadt, Germany). In this study, all chemicals were of analytical grade.

Specimen Preparations

The Kumpang wood was cut into three sections 1.2 m long. Each bolt was quarter-sawn to produce planks 4 cm thick and subsequently conditioned to air drying in a room with 60% relative humidity and an ambient temperature of 25 °C for one month prior to testing. The planks were ripped and machined to 340 mm (L) x 20 mm (T) x 10 mm (R) for three-point bending and free-free vibration testing.

Preparation of Treated wood (TW)

All the samples were oven dried at 105 °C to constant weight before impregnation. The oven-dried specimens and 5% 4-methyl catechol in 1000 mL methanol at pH levels of 8, 9, 10, and 11 were separately placed in an impregnation vacuum chamber at 75 mm (Hg) for 30 min. These specimens were then removed from the chamber, and excess chemicals were wiped off with a dry cloth. Specimens wrapped with aluminum foil were placed in an oven for 24 h at 105 °C for the polymerization process. When the solid raw wood specimens were treated with a solution of 4-methyl catechol at pH 8, it was named TW at pH 8; at pH 9, it was named TW at pH 9; at pH 10, it was named TW at pH 10; and at pH 11, it was named TW at pH 11.

Test Methods

Determination of weight percentage gain (WPG)

Weight percentage gain (WPG) was calculated using the following equation,

$$WPG (\%) = [(W_f - W_i) / W_i] \times 100 \quad (1)$$

where W_f and W_i are the oven-dried weight of the TW and the raw wood, respectively.

Determination of water uptake (WU)

The oven-dried specimens were immersed in distilled water for fifteen days according to ASTM D570-98 (D570 1985) to measure the water uptake. The increase in the weight of the specimens was calculated using the following equation,

$$WU (\%) = [(W_2 - W_1)/W_1] \times 100 \quad (2)$$

where W_2 is the weight of treated (or untreated control) wood samples after immersion and W_1 is the weight the oven-dried sample, respectively.

Density determination

All specimens were kept in the oven at 103 °C for 72 h before density determination. The oven-dry density of each sample was then determined by using the water immersion method (Bowyer *et al.* 2003). The calculation was as follows:

$$\text{Density} = \text{Mass of wood} / \text{Volume of wood} \quad (3)$$

Fourier transform infrared spectroscopy (FTIR)

The infrared spectra of all specimens were recorded on a Shimadzu FT-IR 81001 Spectrophotometer (Kyoto, Japan). The wavenumber range of the scan used ranged from 4000 to 600 cm^{-1} . The technique used was attenuated total reflection.

X-ray diffraction (XRD) analysis

X-ray diffraction (XRD) analyses for raw wood and treated wood were performed with a Rigaku diffractometer (Tokyo, Japan), operating with Cu $K\alpha$ radiation, wavelength of 0.154 nm, 40 kV, and 30 mA. The XRD crystallinity index (CI_{XRD}) was calculated using the following height ratio of diffraction peaks,

$$CI_{\text{XRD}} (\%) = \frac{I_{002} - I_{\text{am}}}{I_{002}} \times 100 \quad (4)$$

where I_{002} is the maximum intensity of the peak at 2θ at approximately 22° and I_{am} is the minimum intensity above baseline at 2θ at approximately 30°, which corresponds to the crystalline and amorphous parts, respectively. The d -spacing between the [002] lattice planes (d_{002}) of the sample was calculated using the Bragg equation,

$$d_{002} = \frac{n\lambda}{2 \sin \theta} \quad (5)$$

where λ is the X-ray wavelength (0.154 nm).

Scanning electron microscopy (SEM)

Fractured surfaces were examined to investigate the interfacial bonding between the wood cell and polymer with filler. These surfaces were imaged using a Hitachi TM3030 scanning electron microscope (SEM) supplied by JEOL (Tokyo, Japan). The SEM specimens were sputter-coated with gold by using JFC- 1600, Tokyo, Japan, prior to observation. The micrographs were acquired at a magnification of 1500.

Modulus of rupture (MOR), modulus of elasticity (MOE), and dynamic Young's modulus (E_d) measurements

Determination of MOE, and MOR were carried out according to ASTM D-143 (2006). Three-point bending tests were conducted using a Shimadzu MSC-5/500 universal testing machine (Kyoto, Japan) operating at a crosshead speed of 5 mm/min. The modulus of rupture (MOR) and modulus of elasticity (MOE) were calculated as follows:

$$MOR = 1.5LW / bd^2 \quad (6)$$

$$MOE = L^3m / 4bd^3 \quad (7)$$

where W is the ultimate failure load, L is the span between the centers of support, b is the mean width (tangential direction) of the sample, d is the mean thickness (radial direction) of the sample, and m is the slope of the tangent to the initial line of the force displacement curve.

Determinations of the dynamic Young's modulus (E_d) for all specimens were carried out using a free-free flexural vibration testing system. The E_d was calculated from the resonant frequency using the following equation,

$$E_d = (4\pi^2 f_n^2 l^4 A \rho) / (I m_n^4) \quad (8)$$

where I is the second moment of area of the beam's cross-section (which is equal to $bd^3/12$), d is the beam's depth, b is the beam's width, l is the beam's length, f_n is the beam's natural frequency at the n^{th} flexural mode, ρ is the beam's density, A is the beam's cross-sectional area, and m_n is a constant related to the free-free beam vibration at the n^{th} flexural mode. The value of m_n at the first mode ($n = 1$) is 4.730 (*i.e.*, $m_1 = 4.730$).

Thermogravimetric analysis (TGA)

Thermogravimetric analysis (TGA) measurements were performed on 5- to 10-mg samples at a heating rate of 10 °C/min in a nitrogen atmosphere using a thermogravimetric analyzer (Model SDT Q600, TA Instruments, Selangor, Malaysia). The thermal decomposition of each sample occurred within a programmed temperature range from 30 to 600 °C under a constant nitrogen flow rate of 5 mL/min. The continuous weight loss and temperature were recorded and analyzed.

RESULTS AND DISCUSSION

Weight Percentage Gain (WPG) and Water Uptake (WU)

Table 1 shows the weight percentage gain (WPG) and the water uptake (WU). As can be seen in Table 1, the TW at pH 8 and pH 9 showed higher WPG compared with raw wood. This higher WPG was due to the –OH group of polymerized 4-methyl catechol that created the covalent bonding with the –OH groups of the wood cell wall (reflected in FTIR analysis) (Rahman et al 2010b). The weight of the degraded hemicellulose and lignin from wood were lower compared with the weight that was added by the polymerized 4-methyl catechol in wood. At pH 8 and pH 9, strong polymerization took place between 4-methyl catechol and the wood cell wall (reflected in the SEM morphology). At pH 10 and pH 11, the weights of the TW were lower than raw wood due to the removal of hemicellulose and lignin, and less polymerization of 4-methyl catechol occurred in the wood.

The TW treated with 4-methyl catechol absorbed less water compared with raw wood because of the removal of hemicellulose and lignin (Hossain *et al.* 2014). The raw wood exhibited a higher percentage of water absorption followed by the TW at pH 11, pH 10, pH 9, and pH 8. This higher percentage was attributed to the fact that 4-methyl catechol solution at a lower pH filled the maximum number of lumens and tracheids of wood and then became polymerized.

Table 1. WU (%) and WPG (%) of the Raw Wood *

Samples	WPG (%)	WU (%)
RW	-	80 ± 10.25
TW at pH 8	20.6	60 ± 5.34
TW at pH 9	17.16	70 ± 5.40
TW at pH 10	-1.1	72.5 ± 7.90
TW at pH 11	-6	76.3 ± 9.30

* Values represent means of 10 replicates

The void area on the wood surface facilitates the water penetration into wood cell walls with hydrophilic hydroxyl groups. At higher pH levels, the hemicellulose and lignin were reduced, and the water absorption was decreased compared with raw wood, as reflected in the SEM and XRD measurements.

FTIR

The Fourier transform infrared spectroscopy (FTIR) spectra of the untreated and treated woods are shown in Fig. 1. The functional groups obtained by FTIR measurements are shown in Table 2.

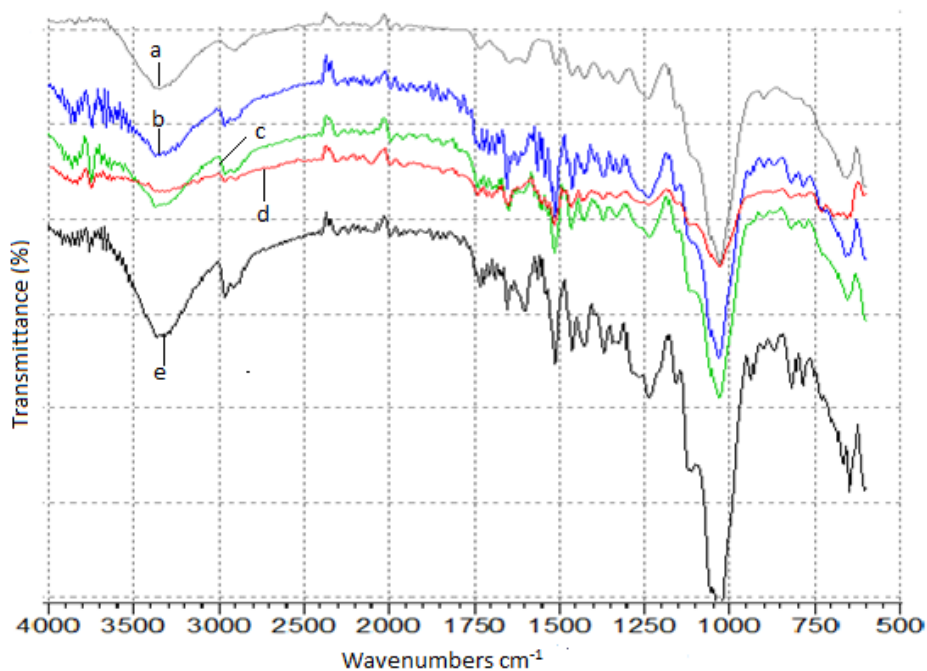


Fig. 1. The FTIR of a) raw wood, b) TW at pH 11, c) TW at pH 10, d) TW at pH 9, and e) TW at pH 8

The broad peak from 3,600 to 3,200 cm^{-1} is associated with $-\text{OH}$ stretching in hydroxyl groups from cellulose (Rahman *et al.* 2010a). Moreover, the relative intensities of TW at pH 8 and pH 9 increased compared with raw wood. This was due to the 4-methyl catechol itself, where $-\text{OH}$ groups appeared in the treated wood. In the presence of NaOH, 4-methyl catechol polymerized with itself. At pH 10 and 11, the relative intensities of the $-\text{OH}$ bands of the TW decreased compared with raw wood. The TW at

pH 10 and pH 11 had more hemicellulose reduction compared with the TW at pH 8 and pH 9. The wavelength from 3750 to 3600 cm^{-1} originated from the $-\text{OH}$ stretching of 4-methyl catechol in the TW whereas the raw wood did not represent this peak (Karpagasundari and Kulothungan 2014). The TW showed more than one peak between 1745 and 1690 cm^{-1} , but raw wood displayed one peak at 1,735 cm^{-1} which indicated that the TW contained different types of carbonyl groups. This peak was due to the conversion of the aromatic ring of 4-methylcatechol to aliphatic alkene (Jha and Halada 2011). The absorbance at 1510 cm^{-1} corresponded to the benzene ring stretching vibration in lignin (Chen *et al.* 2010).

Compared with the raw wood, the absorption band at 1060 cm^{-1} decreased in TW above pH 8. This indicated that the 4-methyl catechol solution in pH levels over 8 reduced the C–O–C bond formation by removing some of the hemicellulose. The reaction between the $-\text{OH}$ in 4-methyl catechol and the $-\text{OH}$ in the wood cell wall produced a C–O–C bridge between them, which shown in Fig. 2.

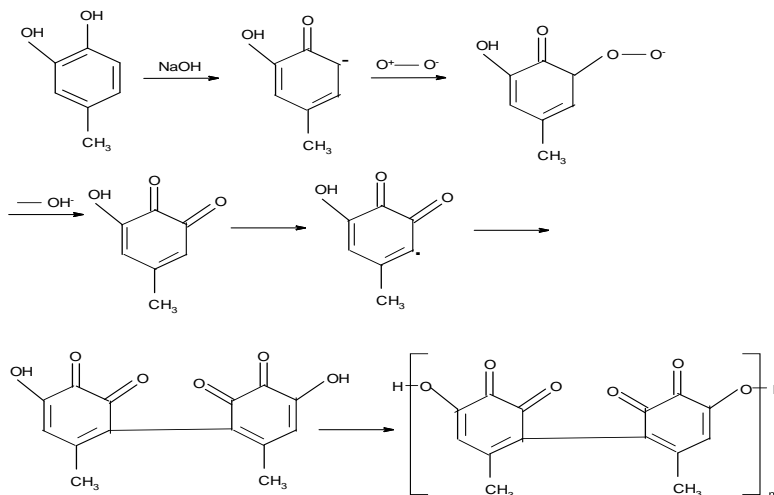
According to the finding, networking between the polymerized 4-methyl catechol and the wood cell wall was better for the TW at pH 8, followed by the TW at pH 10 and pH 11. In addition, the absorbance at 1,600 cm^{-1} by the aromatic skeletal stretching vibration in lignin was reduced in the TW at pH 10 and pH 11, which may be attributed to the degradation of lignin (Xiao *et al.* 2012).

Table 2. Functional Groups Obtained from FTIR Measurements of NaOH-Influenced 4-Methyl Catechol-Treated Wood

Wavelength range (cm^{-1})	Assignment
3600 to 3000	$-\text{OH}$ stretching cellulose, hemicellulose, lignin
3750 to 3600	$-\text{OH}$ stretching of catechol
2900 to 2800	CH stretching
1735 to 1740	C=O, carbonyl group
1600	Aromatic skeletal stretching vibration
1650	Alkene group
1060	C–O–C stretching

The reaction scheme

a) Polymerization of 4-methyl catechol:



b) Wood and polymerized 4-methyl catechol reaction:

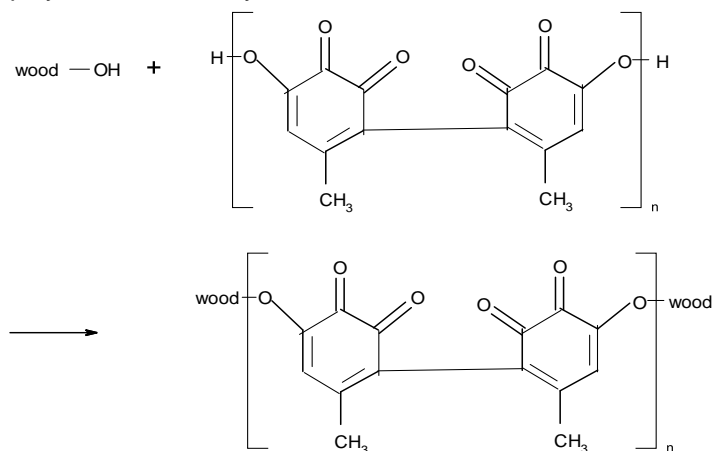


Fig. 2. Schematic reaction mechanism of a) polymerization of 4-methyl catechol and b) wood with polymerized 4-methyl catechol

XRD

The X-ray diffractogram of raw wood and the TW at various pH levels is shown in Fig. 3. The diffraction pattern showed two main peaks for cellulose in the TW and the raw wood.

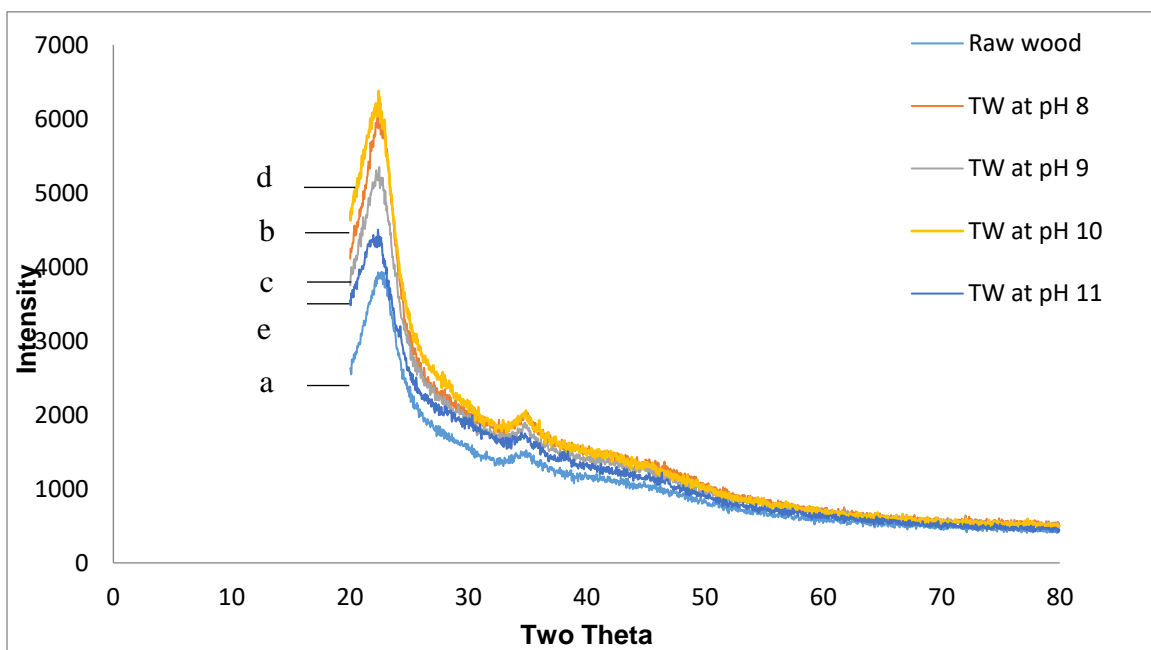


Fig. 3. X-ray diffraction (XRD) diffractograms of a) raw wood, b) TW at pH 8, c) TW at pH 9, d) TW at pH 10, and e) TW at pH 11

The X-ray intensity was measured in the range of 20 theta to 80 theta due to the clear peak intensity would be shown within this temperature range (Zhang and Wang 2007). The peak observed at $2\theta = 22.4^\circ$ assigned to the [002] crystalline plane was used to calculate the CI_{XRD} (Wada *et al.* 2004). The peak at $2\theta = 36^\circ$ showed [040] crystalline

planes. According to the finding, the 2θ value of the raw wood was higher than that of the TW. The d -spacing of the TW at the [002] plane was higher than in the raw wood. This difference established that the wood sample had been effectively treated by polymer. The changes in the diffractograms of the TW were analyzed in order to determine the crystallinity index (CI); these values are reported in Table 3. The CI_{XRD} value of the TW at pH 8 was higher, followed by the TW at pH 9, pH 10, pH 11, and raw wood, respectively (Chen *et al.* 2010). The resulting values are due to the removal of wax, hemicellulose, and pectin from wood, and the decrease in amorphous movement of the wood cell wall by polymerized 4-methyl catechol at lower pH levels (Howell *et al.* 2009; Agubra *et al.* 2013). There was no extra peak with respect to the raw wood. The lack of peaks resulted because the polymerized 4-methyl catechol only filled the wood cavities in the wood's surface and did not form a strong polar bond with them.

Table 3. Crystallinity Index (CI_{XRD}) and d -Spacing as Obtained by XRD Measurements on NaOH-Influenced 4-Methyl Catechol-Treated Wood

Sample	CI_{XRD} (%)	2θ (002)	d -Spacing (002)
Raw wood	66.59	22.6967	0.3913
TW at pH 8	72.49	22.4657	0.3976
TW at pH 9	72.16	22.3337	0.3953
TW at pH 10	69.64	22.4327	0.3959
TW at pH 11	65.8	22.3667	0.3970

Scanning Electron Microscopic Analysis (SEM)

The scanning electron micrographs of raw wood and various TW at different pH levels are shown in Figs. 4a, 4b, 4c, 4d, and 4e.

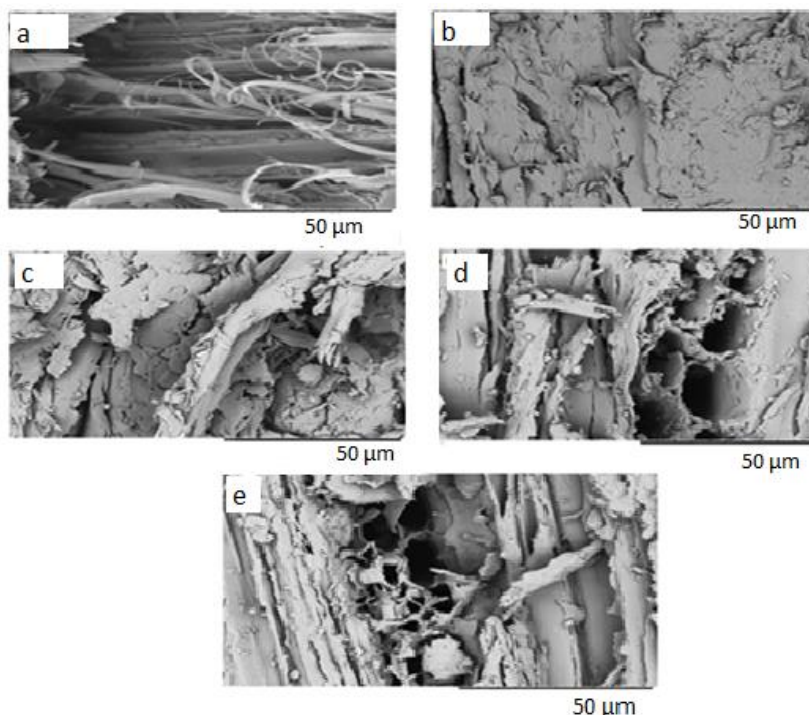


Fig. 4. SEM images of a) raw wood, b) TW at pH 8, c) TW at pH 9, d) TW at pH 10, and e) TW at pH 11

The lumen and tracheids of the wood were filled by the solid polymers of 4-methyl catechol. In Figs. 4d and 4e, the TW at pH 10 and pH 11 showed rough surfaces compared with the RW at pH 8 and pH 9. This contrast was due to more degradation of the cementing hemicellulose and lignin (Hajiha *et al.* 2014; Stevulova *et al.* 2014). As can be seen in Figs. 4b and 4c, the TW at pH 8 and pH 9 showed smoother surfaces due to the polymerized 4-methyl catechol, which filled the voids and the cavities. The poor interaction between the polymer and the wood implied a more brittle composite (Li *et al.* 2011). From the SEM results it can be concluded that 4-methyl catechol was more polymerized at pH 8 and pH 9 compared with polymerization at pH 10 and pH 11.

MOR, MOE, and E_d

The MOE, MOR, and E_d analyses of the raw wood and the TW are shown in Table 4. The TW at pH 8, pH 9, and pH 10 showed higher MOE and MOR compared with raw wood due to the polymerized 4-methyl catechol that formed the covalent bonds with the wood cell wall. Under alkaline conditions, the hydrogen bond structure of wood ruptured when the concentrated alkali permeated into the fiber from outside to inside (Zheng *et al.* 2012). The proportion of intra-molecular hydrogen bonds increased, while the proportion of total intermolecular hydrogen bonds decreased (Xu *et al.* 2016). Consequently, it was expected that more hydroxyl groups would be exposed after the rupture of hydrogen bonds and the cohesion of the fiber would decrease, thus increasing the disintegration of the fiber performance of raw wood (Villasante *et al.* 2013; Boonstra *et al.* 2007). 4-Methyl catechol was also encouraged to react with the –OH group of the wood cell wall to form covalent bonds. Thus, the MOE and MOR of the alkali-influenced TW increased compared with the raw wood. Polar carbonyl groups and the –OH group of polymerized 4-methyl catechol created dipole bonds with the polar group of the wood cell wall (Jha and Halada 2011). The non-polar cyclic parts of the polymerized 4-methyl catechol produced van der Waals forces with the non-polar lignin material of wood. Consequently, the MOE and MOR of the TW at pH 8, pH 9, and pH 10 increased compared with raw wood. The MOR and MOE of the TW at pH 11 was the lowest among both the TW and the raw wood. This result occurred because the NaOH solution at a higher pH degraded more cementing hemicellulose and lignin than it did at lower pH solutions.

Table 4. MOE, MOR, and E_d of Raw Wood and Treated Wood

Samples	MOE (GPa)	MOR (MPa)	E_d (GPa)
RW	6.29 ± 3.05	55.21 ± 25.16	13.30 ± 2.56
TW at pH8	13.54 ± 2.48	99.96 ± 3.60	24.50 ± 3.52
TW at pH9	13.10 ± 3.25	97.13 ± 15.35	20.20 ± 5.48
TW at pH10	9.45 ± 2.21	91.35 ± 14.13	17.18 ± 3.55
TW at pH11	4.72 ± 2.90	71.12 ± 15.98	13.88 ± 3.21

* Values represent means of 10 replicates.

Among the TW and raw wood, the E_d of TW at pH 8 was highest, followed by TW at pH 9, pH 10, pH 11, and raw wood, respectively. This was due to the densities of TW which were higher compared to raw wood. High density increases the shearing force in wood composite (Islam *et al.* 2012b). In the presence of shearing force, the free energy increases and thus the molecules continuously oscillate (Toh 1979). The shearing force varies sinusoidally with time. The E_d of raw wood was slightly lower than TW at pH 11 as more hemicellulose and lignin were removed from wood by NaOH, which reduced the density. This result demonstrated that cellulose and 4-methyl catechol bonding had improved the E_d in the absence of hemicellulose and lignin.

Thermogravimetric Analysis (TGA)

The thermal stability of raw wood and wood treated with 4-methyl catechol at various pH levels is shown in Fig. 5. Raw wood, TW at pH 10, and TW at pH 11 showed two steps of thermal degradation and decomposition. However, TW at pH 8 and TW at pH 9 showed three steps of thermal degradation and decomposition (shown in Table 5). The first step of weight loss for both raw wood and TW occurred between 32 and 126 °C for the evaporation of absorbed moisture (Liu *et al.* 2013). The initial weight loss below 126 °C was the lowest for TW at pH 8, compared with TW at pH 9, TW at pH 10, raw wood, and TW at pH 11, respectively. At pH 8, polymerization of 4-methyl catechol was optimum compared with pH 9, pH 10, and pH 11. This was due to the removal of lignin and hemicellulose at higher pH levels. Therefore, the tendency to liberate moisture upon heating would be minimum for TW at pH 8 (Das and Chakraborty 2006).

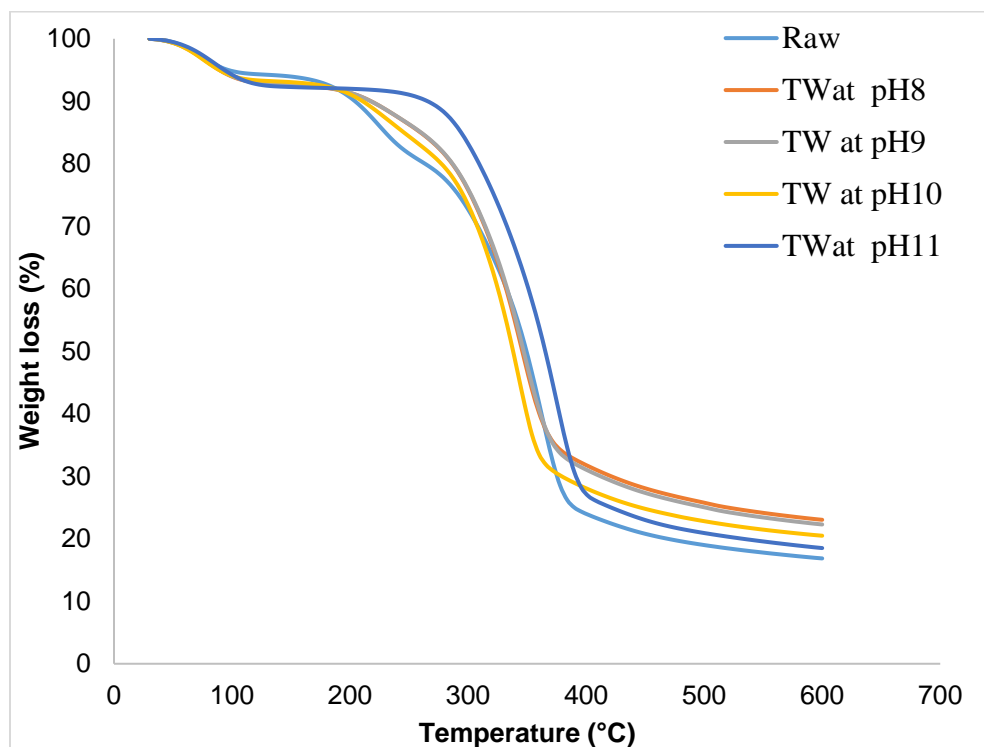


Fig. 5. TGA of a) raw wood, b) TW at pH 11, c) TW at pH 10, d) TW at pH 9, and e) TW at pH 8

The second step of decomposition occurred between 110 and 282 °C, in which the decomposition of the hemicellulose of raw wood and TW occurred (Marques *et al.* 2015). In this temperature range, TW at pH 8 were less stable thermally compared with other treated wood. The TW at pH 8 contained higher hemicellulose followed by pH 9, pH 10, and pH 11, respectively. Thus, TW at higher pH levels were more stable thermally compared with lower pH levels. This was due to varying amounts of hemicellulose in TW at different pH levels.

The third step of decomposition occurred between 282 and 400 °C. This step occurred in order to break the bonds between wood (cellulose, lignin) and 4-methyl catechol. This step released combustible gases such as carbon monoxide, hydrogen, and methane, as well as carbon dioxide and tars that predominate as the temperature rises (Tomczak *et al.* 2007; TranVan *et al.* 2014). In this stage, TW at pH 8 were thermally more stable than TW at pH 9, because of cellulose–O–4–methyl catechol bonding in the glycoside chain.

The residual weight was higher for TW at pH 11 compared with the residual weight of TW at pH 10, TW at pH 9, raw wood, and TW at pH 8, respectively. This difference was due to the increasing pH for the 4-methyl catechol solution, which led to the formation of the lignin–cellulose complex (Ray *et al.* 2002). The residual weight of TW at pH 8 was lower than raw wood due to the presence of unstable cyclic diene in polymerized 4-methyl catechol.

Table 5. Results of TG Analysis for Raw Wood and TW

Sample Name	Stage of Transition	Transition Temperature			Weight loss at corresponding transition (%)	Residual weight (%) at 3rd stage transition
		T_i	T_m	T_f		
Raw wood	1st	37	80	121	7.30	24.81
	2nd	127	354	425	67.65	
TW at pH 8	1st	32	71	124	5.7	20.51
	2nd	125	224	264	14.29	
	3rd	267	351	459	59.12	
TW at pH 9	1st	35	73	121	6.5	24.4
	2nd	172	250	294	16.41	
	3rd	298	341	461	50.39	
TW at pH 10	1st	38	75	119	6.79	28.57
	2nd	128	334	433	64	
TW at pH 11	1st	36	75	125	7.03	31.22
	2nd	133	330	409	61	

T_i : Onset temperature

T_m : Temperature corresponding to the maximum rate of mass loss

T_f : End temperature

CONCLUSIONS

1. By studying FTIR, TGA, XRD, and SEM, it was concluded that wood was treated by 4-methyl catechol in the presence of NaOH.
2. The CI_{XRD} of the 002 plane of TW at pH 8 was more crystalline compared to TW at other pH level.

3. The SEM micrographs showed that TW at pH 8 and TW at pH 9 had smoother surfaces compared with TW at pH 10, TW at pH 11, and raw wood.
4. The TW at pH 8 had higher MOE, MOR, and E_d , followed by TW at pH 9, TW at pH 10, TW at pH 11 and raw wood, respectively.
5. Raw wood gained weight after being treated by 4-methyl catechol at both pH 8 and pH 9, while it (raw wood) lost its weight at both pH 10 and pH 11.
6. Water uptake by TW at pH 8 was the lowest among all the treated wood and raw wood because solution at a lower pH entered into maximum number of lumen and tracheids of wood and then it (4-methyl catechol) was polymerized.
7. The TGA results showed that between 267 and 400 °C, TW were less stable thermally than raw wood due to the presence of unstable cyclic diene in polymerized 4-methyl catechol.

ACKNOWLEDGMENTS

This work was financially supported by University of Malaysia Sarawak under the grant number FRGS/SG02 (01)/1085/2013(31).

REFERENCES CITED

- Agubra, V. A., Owuor, P. S., and Hosur, M. V. (2013). "Influence of nanoclay dispersion methods on the mechanical behavior of E-glass/epoxy nanocomposites," *Nanomaterials* 3(3), 550-563. DOI: 10.3390/nano3030550
- ASTM D-143 (2006). "Standard method of testing small clear specimens of timber," American Society for Testing and Materials, USA.
- Barreto, A. C. H., Rosa, D. S., Fechine, P. B. A., and Mazzetto, S. E. (2011). "Properties of sisal fibers treated by alkali solution and their application into cardanol-based biocomposites," *Composites Part A: Applied Science and Manufacturing* 42(5), 492-500. DOI: 10.1016/j.compositesa.2011.01.008
- Belgacem, M. N., and Gandini, A. (2008). "Chemical modification of wood," in: *Monomers, Polymers and Composites from Renewable Resources*, M. N. Belgacem and A. Gandini (eds.), Elsevier, Amsterdam, Netherlands, pp. 419-430. DOI: 10.1016/B978-0-08-045316-3.00020-X
- Boonstra, M. J., Acker, J. V., Tjeerdsma, B. F., and Kegek, E. V. (2007). "Strength properties of thermally modified softwoods and its relation to polymeric structural wood constituents," *Annals of Forest Science* 64, 679-690.
- Bowyer, J. L., Shmulsky, R., and Haygreen, J. G. (2003). *Forest Products and Wood Science - an Introduction*, Fourth Ed., Iowa State University Press, Ames.
- Chen, H., Ferrari, C., Angiuli, M., Yao, J., Raspi, C., and Bramanti, E. (2010). "Qualitative and quantitative analysis of wood samples by Fourier transform infrared and multivariate analysis," *Carbohydrate Polymers* 82(3), 772-778. DOI: 10.1016/j.carbpol.2010.05.052
- Das, M., and Chakrabarty, D. (2006). "Influence of alkali treatment on the fine structure and morphology of bamboo fibers," *Journal of Applied Polymer Science* 102(5),

- 5050-5056. DOI: 10.1002/app.25105
- Das, M., and Chakrabarty, D. (2008). "Thermogravimetric analysis and weathering study by water immersion of alkali-treated bamboo fiber," *BioResources* 3(4), 1051-1062. DOI: 10.15376/biores.3.4.1051-1062
- Devi, R. R., and Maji, T. K. (2013). "In situ polymerized wood polymer composite: Effect of additives and nanoclay on the thermal, mechanical properties," *Materials Research* 16(4), 954-963. DOI: 10.1590/S1516-14392013005000071
- Esteves, B., Nunes, L., Domingos, I., and Pereira, H. (2014). "Improvement of termite resistance, dimensional stability and mechanical properties of pine wood by paraffin impregnation," *European Journal of Wood and Wood Products* 72(5), 609-615. DOI: 10.1007/s00107-014-0823-7
- Ghali, L., Msahli, S., Zidi, M., and Sakli, F. (2009). "Effect of pre-treatment of luffa fibres on the structural properties," *Materials Letters* 63(1), 61-63. DOI: 10.1016/j.matlet.2008.09.008
- Glasser, W. G., Taib, R., Jain, R. K., and Kander, R. (1999). "Fiber-reinforced cellulosic thermoplastic composites," *Journal of Applied Polymer Science* 73(7), 1329-1340. DOI: 10.1002/(SICI)1097-4628(19990815)73:7<1329::AID-APP26>3.0.CO;2-Q
- Hossain, M. F., Islam, M. K., and Islam, M. A. (2014). "Effect of chemical treatment on the mechanical and physical property of wood saw dust particles reinforced polymer matrix composites," *Procedia Engineering* 90, 39-45. DOI: 10.1016/j.proeng.2014.11.811
- Howell, C., Hastrup, A. C. S., Goodell, B., and Jellison, J. (2009). "Temporal changes in wood crystalline cellulose during degradation by brown rot fungi," *International Biodeterioration and Biodegradation* 63(4), 414-419. DOI: 10.1016/j.ibiod.2008.11.009
- Islam, M. S., Hamdan, S., Rusop, M., Rahman, M. R., Ahmed, A. S., and Idrus, M. A. M. (2012a). "Dimensional stability and water repellent efficiency measurement of chemically modified tropical light hardwood," *BioResources* 7(1), 1221-1231. DOI: 10.15376/biores.7.1.1221-1231
- Islam, M. S., Hamdan, S., Talib, Z. A., Ahmed, A. S., and Rahman, M. R. (2012b). "Tropical wood polymer nanocomposite (WPNC): The impact of nanoclay on dynamic mechanical thermal properties," *Composites Science and Technology* 72(16), 1995-2001. DOI: 10.1016/j.compscitech.2012.09.003
- Jha, P. K., and Halada, G. P. (2011). "The catalytic role of uranyl in formation of polycatechol complexes," *Chemistry Central Journal* 5(12), DOI: 10.1186/1752-153X-5-12
- Junior, D. L., Colodette, J. L., and Gomes, V. J. (2010). "Extraction of wood hemicelluloses through NaOH leaching," *Cerne* 16(4), 423-429. DOI: 10.1590/S0104-77602010000400001
- Karpagasundari, C., and Kulothungan, S. (2014). "Analysis of bioactive compounds in *Physalis minima* leaves using GC MS, HPLC, UV-VIS and FTIR techniques," *Journal of Pharmacognosy and Phytochemistry* 3(4), 196-201.
- Kojiro, K., Furuta, Y., and Ishimaru, Y. (2008). "Influence of heating history on dynamic viscoelastic properties and dimensions of dry wood," *Journal of Wood Science* 54(3), 196-201. DOI: 10.1007/s10086-007-0942-4
- Kollmann, F. P. F., and Côté, W. A. (1968). "Physics of wood," in: *Principles of Wood Science and Technology*, F. P. F. Kollmann and W. A. Côté (eds.), Springer Verlag, Berlin, Germany, pp. 185-186.

- Ku, H., Wang, H., Pattarachaiyakoo, N., and Trada, M. (2011). "A review on the tensile properties of natural fiber reinforced polymer composites," *Composites Part B: Engineering* 42(4), 856-873. DOI: 10.1016/j.compositesb.2011.01.010
- Landis, E. N., and Navi, P. (2009). "Modeling crack propagation in wood and wood composites. A review. COST Action E35 2004-2008: Wood machining - micromechanics and fracture," *Holzforschung* 63(2), 150-156. DOI: 10.1515/HF.2009.010
- Li, Y. F., Liu, Y. X., Wang, X. M., Wu, Q. L., Yu, H. P., and Li, J. (2011). "Wood-polymer composites prepared by the *in situ* polymerization of monomers within wood," *Journal of Applied Polymer Science* 119(6), 3207-3216. DOI: 10.1002/app.32837
- Liu, Z., Jiang, Z., Fei, B., and Liu, X. (2013). "Thermal decomposition characteristics of Chinese fir," *BioResources* 8(4), 5014-5024. DOI: 10.15376/biores.8.4.5014-5024
- Marques, M. F. V., Melo, R. P., Araujo, R. S., Lunz, J. N., and Aguiar, V. O. (2015). "Improvement of mechanical properties of natural fiber-polypropylene composites using successive alkaline treatments," *Journal of Applied Polymer Science* 132(12), DOI: 10.1002/app.41710
- Mattos, B. D., Cademartori, P. H. G., Lourençon, T. V., Gatto, D. A., and Magalhães, W. L. E. (2014). "Biodeterioration of wood from two fast-growing eucalypts exposed to field test," *International Biodeterioration and Biodegradation* 93, 210-215. DOI: 10.1016/j.ibiod.2014.04.027
- Mohanty, A. K., Misra, M., and Drzal, L. T. (2001). "Surface modifications of natural fibers and performance of the resulting biocomposites: An overview," *Composite Interfaces* 8(5), 313-343. DOI: 10.1163/156855401753255422
- Mohebbi, B., and Miltz, H. (2010). "Microbial attack of acetylated wood in field soil trials," *International Biodeterioration and Biodegradation* 64(1), 41-50. DOI: 10.1016/j.ibiod.2009.10.005
- O'Donnell, A., Dweib, M. A., and Wool, R. P. (2004). "Natural fiber composites with plant oil-based resin," *Composites Science and Technology* 64(9), 1135-1145. DOI: 10.1016/j.compscitech.2003.09.024
- Rahman, M. R., Hamdan, S., Ahmed, A. S., and Islam, M. S. (2010a). "Mechanical and biological performance of sodium metaperiodate-impregnated plasticized wood (PW)," *BioResources* 5(2), 1022-1035. DOI: 10.15376/biores.5.2.1022-1035
- Rahman, M. R., Hamdan, S., Ahmed, A. S., Islam, M. S., Talib, Z. A., Abdullah, W. F. W., and Mat, M. S. C. (2011). "Thermogravimetric analysis and dynamic Young's modulus measurement of *N,N*-dimethylacetamide-impregnated wood polymer composites," *Journal of Vinyl and Additive Technology* 17(3), 177-183. DOI: 10.1002/vnl.20275
- Rahman, M. R., Hamdan, S., Hasan, M., and Talib, Z. A. (2010b). "Structural analysis and dynamic Young's modulus measurement of selected tropical wood polymer composites," *Materials Science and Technology* 26(9), 1073-1078. DOI: 10.1179/174328409X410827
- Rahman, M. R., Hamdan, S., Islam, M. S., and Ahmed, A. S. (2012). "Influence of nanoclay/phenol formaldehyde resin on wood polymer nanocomposites," *Journal of Applied Sciences* 12(14), 1481-1487. DOI: 10.3923/jas.2012.1481.1487

- Ray, D., Sarkar, B. K., Basak, R. K., and Rana, A. K. (2002). "Study of the thermal behavior of alkali-treated jute fibers," *Journal of Applied Polymer Science* 85(12), 2594-2599. DOI: 10.1002/app.10934
- Redman, A. L., Bailleres, H., Turner, I., and Perré, P. (2016). "Characterisation of wood–water relationships and transverse anatomy and their relationship to drying degrade," *Wood Science and Technology* 50(4), 739-757. DOI: 10.1007/s00226-016-0818-0
- Rowell, R. (2012). "Chemical modification of wood to produce stable and durable composites," *Cellulose Chemistry and Technology* 46(7-8), 443-448.
- Sahin, H. T., and Mantanis, G. (2011). "Colour changes in wood surfaces modified by ananoparticulate based treatment," *Wood Research* 56(4), 525-532.
- Singh, S., and Mohanty, A. K. (2007). "Wood fiber reinforced bacterial bioplastic composites: Fabrication and performance evaluation," *Composites Science and Technology* 67(9), 1753-1763. DOI: 10.1016/j.compscitech.2006.11.009
- Stark, N. M., and Rowlands, R. E. (2003). "Effects of wood fiber characteristics on mechanical properties of wood/polypropylene composites," *Wood and Fibre Science* 35(2), 167-174.
- Sultan, M. T., Rahman, M. R., Hamdan, S., Lai, J. C. H. and Talib, Z. A. (2016). "Clay dispersed styrene-co-glycidyl methacrylate impregnated kumpang wood polymer nanocomposites: Impact on mechanical and morphological properties," *BioResources* 11(3), 6649-6662. DOI: 10.15376/biores.11.3.6649-6662
- Toh, H. K. (1979). *A Study of Diffusion in Polymers using C-14 Labelled Molecules*, Ph.D. Dissertation, Loughborough University, Leicestershire, UK.
- Tomczak, F., Sydenstricker, T. H. D., and Satyanarayana, K. G. (2007). "Studies on lignocellulosic fibers of Brazil. Part II: Morphology and properties of Brazilian coconut fibers," *Composites Part A: Applied Science and Manufacturing* 38(7), 1710-1721. DOI: 10.1016/j.compositesa.2007.02.004
- Tran Van, L., Legrand, V., and Jacquemin, F. (2014). "Thermal decomposition kinetics of balsa wood: Kinetics and degradation mechanisms comparison between dry and moisturized materials," *Polymer Degradation and Stability* 110, 208-215. DOI: 10.1016/j.polymdegradstab.2014.09.004
- Villasante, A., Laina, R., Rojas, J. A. M., and Vignote, S. (2013). "Mechanical properties of wood from *Pinus sylvestris* L. treated with light organic solvent preservative and with waterborne copper azole," *Forest Systems* 23(3), 416-422.
- Wada, M., Heux, L., and Sugiyama, J. (2004). "Polymorphism of cellulose I family: Reinvestigation of cellulose IV₁," *Biomacromolecules* 5(4), 1385-1391. DOI: 10.1021/bm0345357
- Xiao, Z., Xie, Y., Adamopoulos, S., and Mai, C. (2012). "Effects of chemical modification with glutaraldehyde on the weathering performance of Scots pine sapwood," *Wood Science and Technology* 46(4), 749-767. DOI: 10.1007/s00226-011-0441-z
- Xu, Y., Wang, J. Qian, X., Zuo, L. and Yue, X. (2016). "Effects of supplementary alkali after alkaline peroxide treatment on the properties of bleached kraft pine fluff pulp," *BioResources* 11(1), 336-353. DOI: 10.15376/biores.11.1.336-353
- Zhang, Z., and Wang Q. (2007). "The new method of XRD measurement of the degree of disorder for anode coke material," *Crystals* 7(5), 1-10.

Zheng, M. X., Li, L. Q., Zheng, M. Y., Wang, X., Ma, H. L., and Wang, K. J. (2012).
“Effect of alkali pretreatment on cellulosic structures of corn stover,” *Environmental
Science and Technology* 35(6), 27-31.

Article submitted: September 5, 2016; Peer review completed: February 6, 2016; Revised
version received and accepted: March 21, 2017; Published: March 29, 2017.
DOI: 10.15376/biores.12.2.3601-3617